DETERMINATION OF APPARENT DIFFUSION COEFFICIENT OF BLOOD AT ITS VARIOUS AGES USING THE TECHNIQUE OF DIFFUSION MRI

NUR HARTINI BINTI MOHD TAIB

UNIVERSITI SAINS MALAYSIA
2010

DETERMINATION OF APPARENT DIFFUSION COEFFICIENT OF BLOOD AT ITS VARIOUS AGES USING THE TECHNIQUE OF DIFFUSION MRI

by

NUR HARTINI BINTI MOHD TAIB

Thesis submitted in fulfillment of the requirements for the Degree of
Master of Science

UNIVERSITI SAINS MALAYSIA
MAY 2010

ACKNOWLEDGEMENTS

Above all, all praises to Allah SWT for giving me the strength and help to complete this thesis. I am indebted to many people who have assisted me in this research.

I have been fortunate to have reaped the benefits of wisdom from my supervisor, Assoc. Prof. Dr. Wan Ahmad Kamil Wan Abdullah. I am very grateful for his support, advice, help and guidance during my master study in USM and in the completion of this thesis. I would also like to thank my co supervisor, Assoc. Prof. Dr. Mohd Ezane Aziz for his guidance and insights.

I am particularly indebted to Assoc. Prof. Dr. Rosline Hassan, Head Department of Hematology for her help and advice. Further, I would like to express my deepest gratitude to the radiographer, Mr. Mohd Nordin Mohd Nor for his assistance afforded to me in acquiring all the data images.

I am also grateful to Mr. Ahmad Kamaludin Muhamad, staff of Central Research Lab, Ms. Wan Soriany Wan Md Zain, staff of Hematology Lab, and Mr. Mohd Nadzri Abu Yazid, staff of Microbiology and Medical Pathology Lab for their help and cooperation.

I appreciated, as well, the support from Universiti Sains Malaysia via the Academic Staff Training Scheme throughout the period of my study. This study was also funded by USM Incentive Grant and Short Term Grant.

Special thanks are dedicated to my beloved husband, Muhammad Nur Salihin Yusoff and our daughter, Nurul Iman and son, Muhammad Adib for their sacrifice, support and prayer for me. They have been and will always be my source of inspiration.

I also thank my parents and mother-in-law, our family members and my fellow friends for their prayer, encouragement and support. Finally, thank you to any individuals who have contributed to this research. May God repay your kindness.

TABLE OF CONTENTS

LIST OF TABLES

LIST OF FIGURES

LIST OF ABBREVIATIONS

ADC	Apparent Diffusion Coefficient
CPDA	Citrate-Phosphate-Dextrose-Adenine
DWI	Diffusion-Weighted Image
DWMRI	Diffusion-Weighted Magnetic Resonance Imaging
EPI	Echo Planar Imaging
FLAIR	Fluid Attenuated Inversion Recovery
FOV	Field of View
Hb	Hemoglobin
HUSM	Universiti Sains Malaysia Hospital
MRI	Magnetic Resonance Imaging
PD	Proton Density Weighted Image
PEDD	Proton-Electron Dipole-Dipole
PROPELLER	Periodically Rotated Overlapping Parellel Lines with Enhanced Reconstruction
RBC	Red Blood Cells
RF	Radio Frequency
ROI	Region of Interest
SD	Standard Deviation
SI	Signal Intensity
TE	Time to Echo
TP	Thromboplastin
TR	Repetition Time
T1	Longitudinal relaxation time
T1WI	T1-Weighted Image
T2	Transversal relaxation time
T2WI	T2-Weighted Image
WBC	White Blood Cells

PENENTUAN PEKALI RESAPAN KETARA DARAH PADA PELBAGAI USIANYA YANG BERBEZA MENGGUNAKAN TEKNIK PENGIMEJAN RESONAN MAGNET WAJARAN DIFFUSI

ABSTRAK

Matlamat kajian ini adalah untuk membina plot kalibrasi ADC bagi MRI diffusi dan untuk melihat corak perubahan keamatan isyarat imej MR wajaran T1-, T2-, PD dan FLAIR terhadap masa dalam julat 1 jam hingga 60 hari. Sampel darah segar manusia telah diambil daripada empat sukarelawan dan dibahagikan kepada 3 kategori yang berbeza iaitu darah yang dicampurkan dengan *Citrate-Phosphate-Dextrose-Adenine (CPDA)*, darah yang dicampurkan dengan *thromboplastin* dan darah tanpa rawatan sebagai kawalan. Satu set imej T1WI, T2WI, PD, FLAIR dan DWI didapatkan menggunakan sistem MRI 1.0 Tesla (GE Signa Horizon LX) di Hospital Universiti Sains Malaysia. Pengukuran keamatan isyarat imej T1WI, T2WI, PD dan FLAIR telah dilakukan menggunakan perisian GE ADW 2.0. Pembinaan semula peta ADC dan pengukuran nilai-nilai ADC bagi imej DWI telah dijalankan menggunakan perisian GE ADW 2.0 (Functool). Kajian ini menunjukkan terdapat corak perubahan bererti yang dipamerkan oleh semua jenis imej. Corak perubahan tersebut dapat dilihat dengan ketara pada imej T1WI, PD dan DWI. Secara amnya, lengkung yang diperolehi boleh dibahagikan kepada tiga bahagian. Pertama, keamatan isyarat bagi semua kategori darah tidak banyak berubah terhadap masa pada dua hari pertama. Kedua, perubahan yang bererti dapat dilihat sehingga hari ke 14. Ketiga, dari hari ke 14 dan seterusnya, nilai yang hampir malar dapat dilihat. Imej T2WI dan FLAIR tidak menunjukkan corak perubahan yang sama seperti T1WI, PD dan DWI, sebaliknya mempamerkan corak perubahan baru yang tidak pernah dilihat sebelum ini. Corak perubahan baru yang diperolehi dalam kajian ADC berpotensi untuk digunakan sebagai rujukan untuk situasi pendarahan yang sebenar. Hasil kajian ini menunjukkan plot ADC boleh digunakan sebagai rujukan umum bagi menentukan usia darah beku.

DETERMINATION OF APPARENT DIFFUSION COEFFICIENT OF BLOOD AT ITS VARIOUS AGES USING THE TECHNIQUE OF DIFFUSION MRI

ABSTRACT

The aim of this study is to develop ADC calibration plot in diffusion MRI and to examine the signal intensity trend of MR-weighted T1-, T2-, proton density and Fluid Attenuated Inversion Recovery images as a function of time ranged from 1 hour to 60 days. Fresh human blood samples were drawn from four volunteers and divided into 3 different categories namely, blood mixed with *Citrate-Phosphate-Dextrose-Adenine (CPDA)*, blood mixed with *thromboplastin* and untreated blood as control. A set of T1WI, T2WI, PD, FLAIR and DWI were acquired using 1.0 Tesla MRI system (GE Signa Horizon LX) at Hospital Universiti Sains Malaysia. Measurements of the signal intensity for T1WI, T2WI, PD and FLAIR images were performed using GE ADW 2.0 Software. The reconstruction of the ADC maps and measurement of the ADC values for DWI were carried out using GE ADW 2.0 (Functool) Software. The study demonstrates that there is a significant trend displayed by all types of images. The trend was obviously exhibited in T1WI, PD and DWI. Generally the curves obtained can be divided into three parts. Firstly, during the first two days in which the signal intensity of all blood categories did not very that much against time. Secondly, significant changes were observed until day 14. Thirdly, from day 14 onwards, reasonably constant values were found. For T2WI and FLAIR images, they did not show a similar trend as of T1WI, PD and DWI but exhibited a new trend which was not seen before. The new trend found in ADC study has the potential of being used as reference to real hemorrhagic situations. The present findings indicate that ADC plot may be used as a general reference in determining the age of blood clot.

CHAPTER 1

INTRODUCTION

1.0 Introduction

Over the past two decades, magnetic resonance imaging (MRI) has become an important tool in brain imaging. More recently, various techniques have been introduced which heralded the ability to not only detect pathological states, but to specifically define, locate and evaluate such conditions. Diffusion-Weighted MRI (DWMRI) is one of the examples of functional imaging that is very useful in the study of brain hemorrhage.

DWMRI uses the signal loss associated with the random thermal motion of water molecules in the presence of magnetic field gradients. A parameter (Apparent Diffusion Coefficient, ADC) is derived which reflects directly the translational mobility of the water molecules in the tissues. An application of this technique in the context of neuro-vascular imaging includes the early detection and assessment of hemorrhage in the brain.

However, based on the literature survey, there are no systematic studies done so far to investigate the accuracy and reliability in estimating the age of hemorrhage. MRI images are reported based on the grayscale varieties of the particular anatomical image qualitatively. Then a suggestion is made to determine an anatomical object such as hemorrhage based on the ADC value.

This study will address the necessity to determine the age of hemorrhage in a quantitative manner. The specific purpose is to develop a reference graph of ADC values versus the age of blood. In addition, the grayscale values of the magnetization signal intensity (SI) of a particular

anatomical structure, in this case the blood, will be obtained from a selected type of MR images namely T1-weighted image (T1WI), T2-weighted image (T2WI), proton density (PD) weighted image and fluid attenuated inversion recovery (FLAIR). The expected outcome of this work is to obtain sets of calibration curves to be used as a guide in interpreting MR images of brain hemorrhage.

1.1 Literature Review

There has been an increasing number of DWMRI studies conducted. Generally, these studies were carried out to investigate the feasibility of DWMRI in identifying and localizing infarctions and lesions in patients with strokes.

Studies conducted by Wardlaw *et al.* (2000) and Everdingen *et al.* (1998) for instance, compared the sensitivity of DWMRI with that of conventional MRI techniques by assessing the ADC values measured from the region of interest in the brain. All of the researchers found that the use of DWMRI in identifying and localizing infarctions in stroke patients is indeed feasible. Diffusion-Weighted Image (DWI) was able to locate the infarctions precisely and even to distinguish a new infarctions from the previous lesions. Wardlaw *et al.* (2000) suggested utility of DWI scanning in the detection and assessment of minor strokes up to at least three weeks after the stroke.

In a previous study done by Lutsep *et al.* (1997), they determined the time of stroke onset by assessing the temporal evolution of ADCs and transversal relaxation time (T2) ratios. They measured the ADC values from a region of interest in the center of the area of ischemia and from a matching

location in the uninvolved contralateral brain. T2-Weighted Image (T2WI) intensity values were acquired from the same anatomic locations in the ischemic and contralateral brain. They expressed the T2WI measurements as a ratio, T2 stroke/ T2 normal brain. Lutsep *et al.* (1997) has shown that DWI is a practical and valuable technique in the clinical setting. They suggest that assessment of ADC values, in conjunction with measurements of T2WI signal intensity, allows the time of stroke onset to be determined more accurately.

1.2 Problem Statement

Even though there are many studies conducted in the field of diffusion MRI, apparently no study has been found in the literature survey on the ADC calibration curve to be used as a guide in the determination of the age of brain hemorrhage. Therefore, this quantitative study, especially the development of the ADC calibration plot will be useful for radiologists.

1.3 Objectives

1.3.1 To understand the fundamentals of Diffusion Weighted MR Imaging and other MR-weighted images of blood at its various ages

1.3.2 To develop a systematic ADC calibration plot of blood at its various age ranging from hours to several months

1.3.3 To establish plots of SI versus the age of blood clot in T1-, T2-, PD-weighted images and FLAIR images

1.3.4 To recognize new trends in the study mentioned in 1.3.2 and 1.3.3 above

Functional MRI, in particular DWMRI is still not widely used in Malaysia. Many aspects of the DWMRI technique have to be explored extensively in medical imaging and radiology reporting of hemorrhagic brain. Better diagnosis and age determination can help in the determination of the likelihood of recurrent hemorrhagic tumor, gives better understanding of the mechanism of the bleeding and hence may help guide acute treatment and better clinical management. The scientific values gained from this research are expected to benefit a wide range of professionals including neurologists, radiologists, medical physicists, academicians, radiographers, biomedical engineers and administrators. Last but not least, the patient will also benefit from this study.

CHAPTER 2

FUNDAMENTALS AND APPLICATIONS OF MAGNETIC RESONANCE IMAGING TECHNIQUE

2.1 Fundamentals of MRI

Approximately 80% of all atoms found in human body are hydrogen. Its nucleus consists of a single positively-charged proton which spins, possesses a small magnetic field and is called magnetic moment (Bushong, 2003).

2.1.1 Precession and Larmor Frequency

When a patient is placed in the MRI gantry, a strong external magnetic field, B_o, is applied to the body, the protons align parallel and anti-parallel to the external magnetic field. Protons with higher energy align anti-parallel while more protons on the lower energy level, align parallel to the field.

These magnetic moments of the protons in the opposing directions cancel out each other. But as there are more protons in the lower energy level, those protons are not cancelled. All of the remaining protons add up their forces in the direction of the external magnetic field and result in a net magnetization in direction along the external magnetic field, as depicted in Figure 2.1. The magnetization is called longitudinal magnetization (Bitar *et al.*, 2006; Westbrook *et al.*, 2005; Sprawls, 1995; Schild, 1990).

The movement of the hydrogen nuclei is called ‘precession’. The speed can be measured as precession frequency, that is, how many times the protons precess per second.

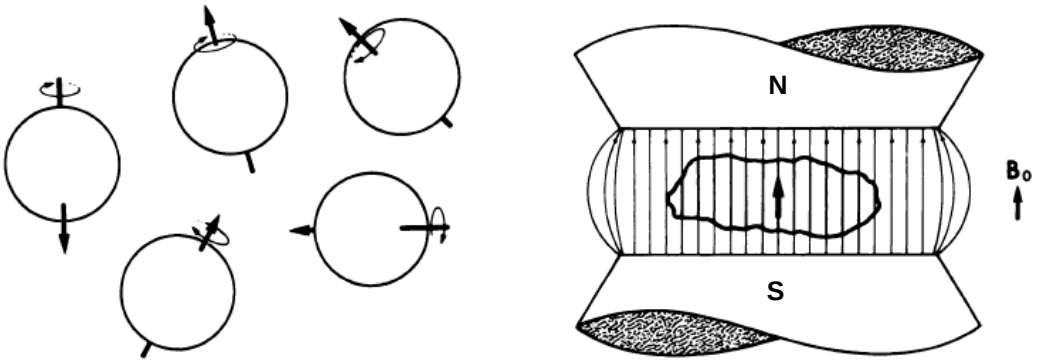

(a) (b)

Figure 2.1: (a) Without external magnetic field, the hydrogen nuclei possess a nuclear spin and spin about their own axis. (b) When external magnetic field, B_o is applied, the magnetic moments align parallel and anti parallel (pointing to north, N and south, S) with the magnetic field, resulting in a net magnetization (Pykett *et al.*, 1982)

In the MRI gantry, all the hydrogen nuclei precess about the z-axis. The precession frequency depends on the strength of the magnetic field. The stronger the magnetic field, the faster the precession rate and the higher the precession frequency. This relationship is described by an equation named Larmor equation, which states that:

$$f = \gamma B_0 \tag{2.1}$$

where f is the precession frequency (MHz), γ is the gyromagnetic ratio (MHz/T) which describes the relationship between the angular momentum and the magnetic moment of each atomic nucleus and B_o is the strength of the external magnetic field, which is given in Tesla (T). The value of γ differs across various atomic nuclei, as shown in Table 2.1 (Prince and Links, 2006; Westbrook *et al.*, 2005).

Table 2.1: Some atomic nuclei and their respective gyromagnetic ratio, γ

NUCLEUS	GYROMAGNETIC RATIO, γ (MHz/T)
^{1}H	42.6
^{19}F	40.1
^{31}P	17.2
^{23}Na	11.3
^{13}C	10.7
^{2}H	6.5
^{17}O	5.8
^{39}K	2.0

2.1.2 RF Excitation and Resonance

When the protons have aligned in direction along the external magnetic field, a short burst of some electromagnetic wave is sent in to the system. The electromagnetic wave is called a radio frequency pulse (RF pulse). Sending in an RF pulse that has the same frequency as the precession frequency of the protons will cause the occurrence of resonance. It causes two effects, that are 1) Some protons absorb energy and thus the amount of longitudinal magnetization decreases. 2) The protons start to precess in phase. Their vectors add up in a direction transverse to the external magnetic field and thus form a transversal magnetization. As a result, signals are generated from the new transversal magnetization (Najarian and Splinter, 2006; Sprawls, 1995; Schild, 1990).

The period between the sending in an RF pulse and sending in the next pulse is called Repetition Time, TR and is measured in millisecond (ms). The period between the sending in an RF pulse and the signal received in the receiver coil is called Echo Time, TE, also measured in ms. When the RF pulse is turned off, the hydrogen nuclei give up their energy, resulting in T1 and T2 Relaxation (Bitar *et al.*, 2006; Westbrook *et al.*, 2005).

2.2 T1, T2 and Proton Density Weighting

2.2.1 Fundamentals

After the RF pulse is switched off, the protons release their energy to the surroundings. They lost their phase coherence and recover their longitudinal magnetization, (M_z). The time that it takes for the longitudinal magnetization to recover to its original value is named *longitudinal relaxation* time, also called *T1* or *spin-lattice relaxation*. The process can be described using the exponential equation below:

$$M_z(t) = M_0\left(1 - e^{-t/T1}\right) \tag{2.2}$$

where $M_z(t)$ is the longitudinal relaxation at time t and M_0 is the magnetization in equilibrium state.

While the longitudinal magnetization increases again, the transversal magnetization (M_{xy}) decreases. The time that it takes for the transversal magnetization to decrease is named *transversal relaxation time,* T2. Another term for transversal relaxation is *spin-spin relaxation*, which also occurs exponentially as:

$$M_{xy}(t) = M_{xy}^{0} e^{-t/T2} \tag{2.3}$$

where M_{xy}^{0} is the initial transverse magnetization and $M_{xy}(t)$ is the transverse magnetization at time t (Wehrli and McGowan, 1996).

T1 relaxation is defined as the time required for the longitudinal magnetization to recover 63% of its maximum whereas T2 relaxation time is the time when transversal magnetization decreased to 37% of its original value. T1 and T2 varies among different body tissues. To acquire a T1-weighted image (T1WI), both TR and TE must be short. On the other hand, to obtain a T2-weighted image (T2WI), both TR and TE must be long. Figure

2.2 shows the exponential relaxation of both longitudinal and transverse magnetization.

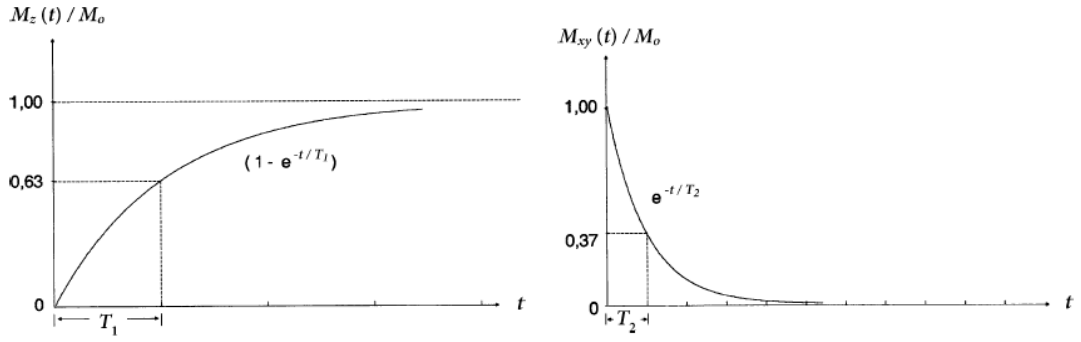

(a) (b)

Figure 2.2: The exponential (a) recovery of M_z, which is T1 Relaxation and (b) decay of M_{xy}, which is T2 Relaxation (Brix *et al.*, 2008)

Proton Density (PD) is the measure of proton concentration (number of protons per unit volume). Net magnetization at equilibrium M_0 and MR signal intensity are proportional to number of proton per unit volume (proton density). Therefore, in order to acquire a PD weighted image, long TR and short TE must be selected to diminish T1 and T2 effects respectively (Westbrook *et al.*, 2005).

2.2.2 Applications

Image weighting and contrast is very important to distinguish between normal and pathological tissues in human body. The most basic form of contrast and most widely used are T1WI, T2WI and PD images (Crooks *et al.*, 1980). In every MR scan conducted, proton density weighting is always present. However, the proton density-weighted image provides little contrast than T1WI and T2WI. As MR image signal intensity is proportional to the number of proton spin in tissues, water content for most tissues in the body is

nearly equivalent, that the proton density for most tissues is quite the same (McRobbie *et al.*, 2003).

T1 and T2 which are based on tissue relaxation times are very sensitive to molecular structure and temperature (Pykett *et al.*, 1982). T1WI and T2WI appearance will change whenever there are changes in the relaxation time of a tissue. Both of these image types have an excellent contrast. T1WI are often thought of as ‘anatomy scans’ as it presents most clearly boundaries between tissues. In T1WI, fluids appear very dark, water-based tissues are mid-grey and fat-based tissues are very bright. Whereas on T2 scans, fluids can be seen very bright while water- and fat-based tissues are mid-grey. T2 images are often thought of as ‘pathology scans’ because collection of abnormal fluid are observed bright against normal tissues which is darker (Mugler III, 2006; McRobbie *et al.*, 2003; Wehrli and McGowan, 1996).

Combination of T1WI, T2WI and PD image as well as other imaging parameters is common in many clinical MR exams in order to achieve the objectives that are not only to detect, but also specifically define, locate and evaluate pathological states (Mugler III, 2006; Wehrli *et al.*, 1998).

2.3 FLAIR Technique

2.3.1 Fundamentals

FLAIR is a variation of the inversion recovery (IR) sequence, which begin with a 180° inverting pulse which is then followed by a 90° pulse (Hornak, 2007). The 180° pulse turns the longitudinal magnetization in the opposite direction. Then, a 90° pulse is sent in to get a transversal

magnetization in order to obtain a measurable signal. The signal that is obtained depends on the time between the 180° and the 90° pulse, which is called Inversion Time (TI) (Schild, 1990).

FLAIR technique nulls signal from fluid by using a very long TI, typically about 2000 ms. By using such a long TI, the longitudinal magnetization of fluid passes its null point, thus little or no longitudinal magnetization is present in the fluid. When the 90° pulse is sent in, the transverse magnetization of fluid is insignificant and therefore no signal is generated from fluid structure (Bitar *et al.*, 2006). The graphical representation of the IR pulse sequence is shown in Figure 2.3.

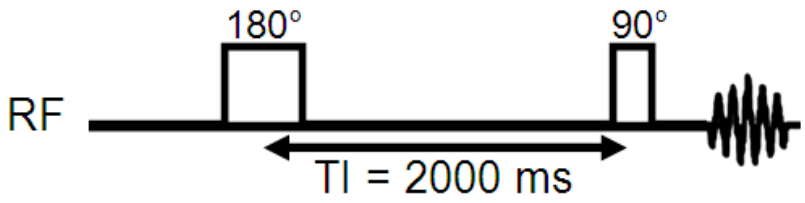

Figure 2.3: The IR pulse sequence, which begin with a 180° RF pulse and followed by a 90° pulse. For FLAIR, a wider range of TI is applied to give a reasonably good fluid suppression (Bitar *et al.*, 2006).

2.3.2 Applications

FLAIR is commonly used in brain and spine imaging as it allows a better diagnosis of preventricular and cord lesions in which the pathological areas may be close to the ventricals. It is also very helpful in the imaging of multiple sclerosis plaques, acute sub-arachnoid hemorrhage and meningitis (Vosegaard, 2005).

2.4 Diffusion Technique

2.4.1 Fundamentals

Molecular diffusion, which is also termed *Brownian motion* is the random motion of molecules from a region of high concentration to that of low concentration, results from the thermal energy carried by the molecules. It is responsible for the transport of water, gases and nutrients in the body, that make diffusion a vital physical process for the normal functioning of living systems (Smalbrock and Chakeres, 1992; Brown and Semelka, 2003).

(a) Pulse Sequence

The most commonly used sequence to produce DWI is the pulse gradient spin echo method, which is also known as Stejskal-Tanner method (Stejskal and Tanner, 1965). This method uses 90°-180° RF pulses with a symmetric pair of large and equal gradient pulses is sent in on either side of the 180° refocusing pulse, as depicted in Figure 2.4. During the first diffusion sensitizing gradient application, each proton starts to precess at unequal rates and lead to spin dephasing. When the second diffusion gradient pulse is sent in, it will cancel the phase shifts by rephasing the spin. If there is no water protons movement during the gradient, the spins will rephase completely. On the other hand, if diffusion occurs, proton spins that move during the gradient pulse will acquire an unequal phase shift resulting in a loss of signal amplitude (Huisman, 2003; Neumann-Haefelin, 2006; Neil, 1997).

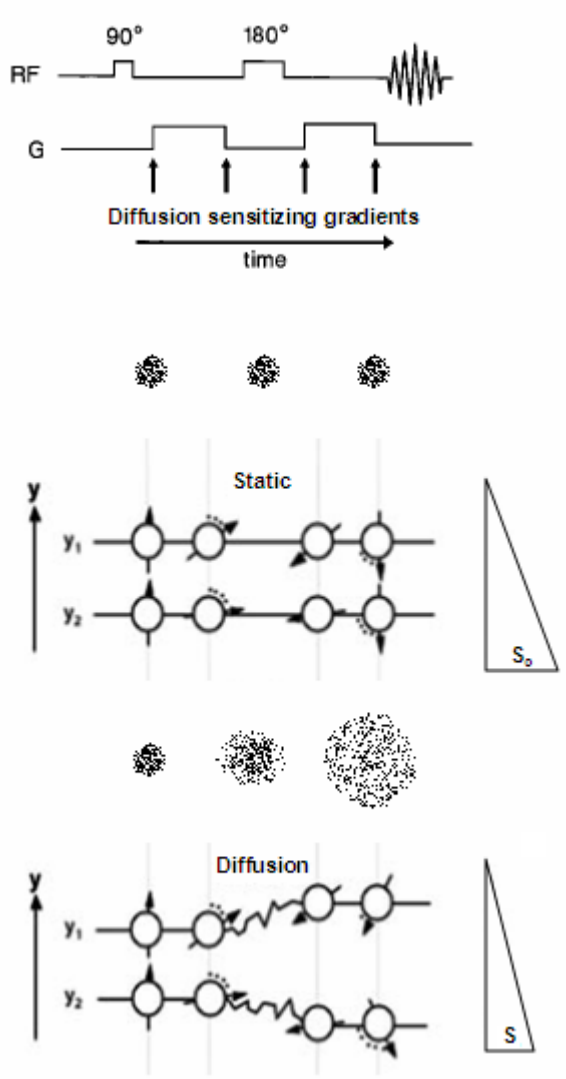

Figure 2.4: The pulse gradient spin echo sequence that is applied for producing DWI. If there is no water protons movement during the gradient, the spins (which are in y direction, y_1 and y_2) will rephase completely and produce the original signal, S_o. On the other hand, if diffusion occurs, proton spins that move during the gradient pulse will acquire an unequal phase shift resulting in a weaker signal, S due to signal loss (Neumann-Haefelin, 2006 and Neil, 1997).

(b) *b*-value

By manipulating some parameters of the pulse sequence shown in Figure 2.5, the degree of weighting which is also termed as *b*-value or *b*-factor can be controlled. The value of *b* which is measured in s/mm^2 is given by

$$b = \gamma^2 G^2 \delta^2 (\Delta - \delta/3) \qquad (2.4)$$

where γ is the gyromagnetic ratio, G is the gradient amplitude, δ is the duration and Δ is the interval of the diffusion sensitizing gradient (Jones, 2005).

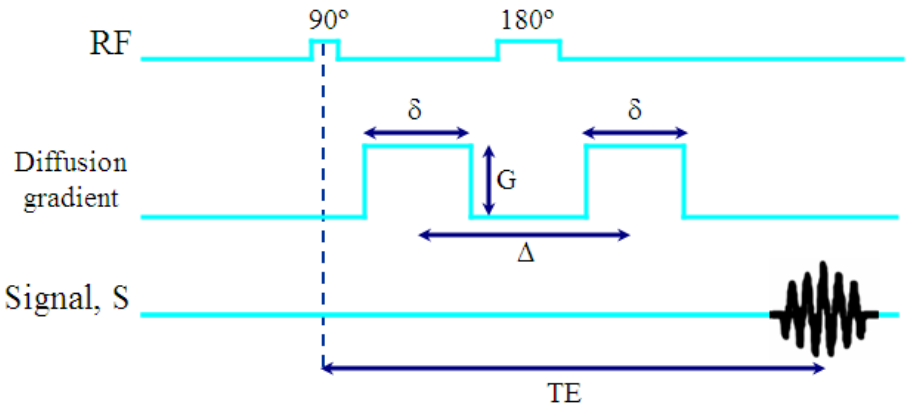

Figure 2.5: The pulse gradient spin echo sequence and its parameters that describe the *b*-value. G is the gradient amplitude, δ is the duration and Δ is the interval of the diffusion sensitizing gradient (Jones, 2005; McRobbie *et al.*, 2003).

(c) Signal Attenuation

As mentioned in Section 2.4.1 (a) and illustrated in Figure 2.4, the diffusing spins during application of the gradient have their phase shifted resulting in an attenuated echo amplitude, thus producing weaker signal, S due to signal loss (Neumann-Haefelin, 2006 and Neil, 1997). The signal loss is characterized by the equation

$$S = S_o \exp(-bD) \tag{2.5}$$

where S and S_o are the signals of the diffusion-weighted and non-diffusion-weighted magnetization respectively, D is the diffusion coefficient and *b* is the *b*-value, a scalar reflecting the properties of the diffusion sensitizing gradient that was present during the experiment.

(d) Apparent Diffusion Coefficient

The average area that molecules can diffuse per unit time is expressed by D, a physical constant named Diffusion Coefficient which has unit of mm^2/s. The diffusion coefficient of pure water is 2.2×10^{-3} mm^2/s. But in body tissues, the diffusion rate of water is influenced by many factors like the microenvironment as well as the energy dependent transportation mechanism. For instance, as for microenvironment factor, *restricted diffusion* occurs, in which the free diffusion of water is impeded by various types of cell membranes with a wide range of permeability. Because of the complicated systems in living tissues, the diffusion coefficient is referred to as *apparent* diffusion coefficient (ADC) (Luypaert *et al.*, 2001; Thomas *et al.*, 2000). A high value of ADC implies high mobility of water and thus, the corresponding ADC map will appear bright (McRobbie *et al.*, 2003; Bihan and Basser, 1995).

(e) ADC map

Maps of the diffusion coefficient can be obtained by acquiring at least two images with different *b* values, that are one with a low *b* value, $b \approx 0$ s/mm^2 (or T2-weighted image) and one with a high *b* value, typically 1000 s/mm^2 or higher. An image obtained using $b \approx 0$ s/mm^2 have very little or no diffusion weighting whereas image acquired with high *b*-value will be heavily diffusion weighted. These images are used for diffusion measurement by fitting the *b*-values into Equation (2.5) as follows:

$$S(TE, b_1) = S_o \exp(-b_1 D) \tag{2.6}$$

$$S(TE, b_2) = S_o \exp(-b_2 D) \tag{2.7}$$

Equations (2.6) and (2.7) show that by keeping TE fixed while changing *b*, the equation below can be created:

$$\frac{S(TE, b_2)}{S(TE, b_1)} = \exp(b_1 - b_2)D \tag{2.8}$$

Taking logarithms of both sides of Equation (2.8) and solving for D yields:

$$D = \frac{1}{b_1 - b_2} \ln\left[\frac{S(TE, b_2)}{S(TE, b_1)}\right] \tag{2.9}$$

The ADC map has an intensity scale which is inverted relative to the DWI used to calculate it. Areas with high mobility of water molecules along the diffusion gradient sampling direction appear dark on the DWI, but bright on the ADC map (Brown and Semelka, 2003; Huisman, 2003; Wheeler-Kingshott *et al.*, 2003; Thomas *et al.*, 2000).

(f) Diffusion MR Imaging with Echo Planar Imaging

Spin–echo Echo Planar Imaging (EPI) is the sequence of choice for Diffusion-Weighted Imaging. Use of this technique permits very fast data acquisition, in which a single echo train is used to collect data from all lines of k-space in one TR (Figure 2.6). The rapidity of EPI acquisition makes it possible to obtain multiple images with many different b-values at a time and enables the generation of the ADC maps with good accuracy.

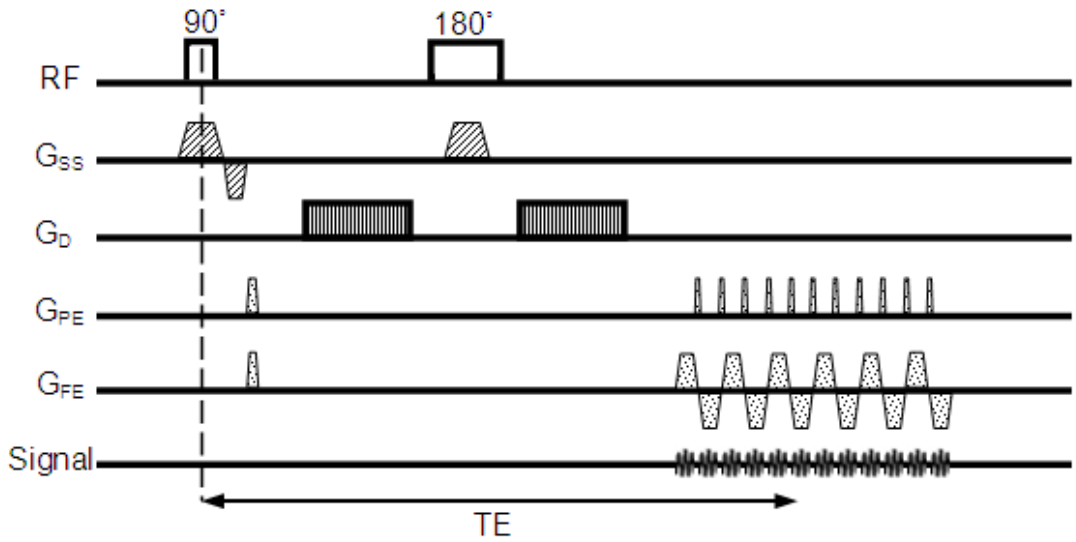

Figure 2.6: Spin-echo EPI DWI sequence. (RF: RF pulse, G_{SS}: Slice selection gradient, G_D: Diffusion gradient, G_{PE}: Phase encoding gradient, G_{FE}: Frequency encoding gradient and TE: Echo time (Turner and Bihan, 1995)

However, there are a number of experimental confounds that are of particular importance for DWI using EPI. As Stejskal-Tanner diffusion sensitizing gradients are put into the conventional MR imaging sequence to sensitize the image to the effect of water molecules mobility, the image become very sensitive to bulk motion, thus more prone to produce artefacts, which will be discussed in the next subtopic (McMahon *et al.*, 2004).

2.4.2 Applications

Although DWMRI is developed quite recently, many studies have proven that this technique has many important clinical values, especially in brain imaging (Moritani *et al.*, 2005; Kummer and Back, 2006; Wilkinson, 2005; Maier *et al.*, 2004; Prichard and Alger, 1999). Complementary to being non-invasive, DWMRI also makes the most of the random, translational motion of water protons in biological tissues, represented by D, reflects the mobility of the water molecules in their microenvironment (Bykowski *et al.*,

2006; Thomas *et al.*, 2000). Consequently, it allows for more accurate diagnosis by producing the ADC maps that makes quantitative measurements available (Steens *et al.*, 2004; Wheeler-Kingshott *et al.*, 2003).

The primary application of DWMRI is in brain hemorrhage (Johnson, 2006; Orakcioglu *et al.*, 2005; Prakash *et al.*, 2004; Dul and Drayer, 1994), stroke (Wardlaw and Farrall, 2004; Rosenbaum, 2000; Schaefer *et al.*, 2000; Wardlaw *et al.*, 2000; Roberts and Rowley, 2002), tumors (Desbarats *et al.*, 2003; Herneth *et al.*, 2002), multiple sclerosis (Wilson *et al.*, 2001; Schaefer *et al.*, 2000), schizophrenia (Maier *et al.*, 2004), intracranial infections (Fillipi, 2005) and traumatic brain injury (Pickard, 2005).

2.5 Artefacts

There are several image artefacts and pitfalls in MRI worthy of consideration and whenever possible it is necessary to reduce or to eliminate them. Some of the artefacts relevant to this work are described below.

2.5.1 Acquisition-Related Artefacts

(a) Wraparound Artefacts

One of the most common artifacts is wraparound, as shown in Figure 2.7. The artefacts arise whenever the anatomy extends outside the field of view (FOV) and being produced at the opposite edge of the image in the phase-encoding direction. The wrapped-in image can overlay the real anatomy being scanned and disturb the image interpretations. This phenomenon is a signal processing artefacts and also known as *aliasing,*

which occurs because the data are not sampled in a continuous, but discrete fashion.

Increasing the FOV in the phase-encode direction may help to prevent the artefacts. However, this will cause a loss of spatial resolution, unless the matrix size is also increased. The larger matrix size will in turn increase the scan time and improve the signal-to-noise ratio (Storey, 2006; McRobbie *et al.*, 2003).

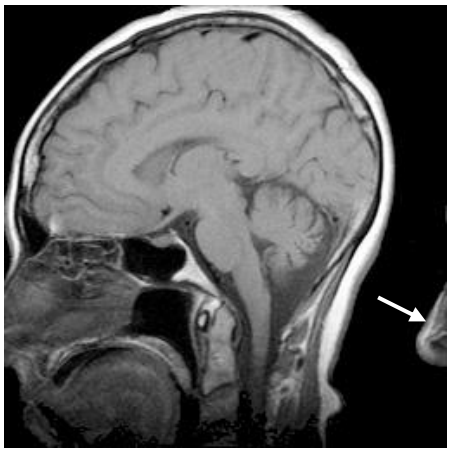

Figure 2.7: Sagittal image of the head contain wraparound artefacts (see the arrows) (Hornak, 2007)

2.5.2 Technique-Specific Artefacts

(a) Eddy Current Artefacts

Eddy currents are electrical currents induced in a conductor by rapid switching of very strong magnetic field gradients. The artefacts are mostly severe when gradients are turned on and off rapidly as in EPI pulse sequence which leads to image distortion and misregistration (Figure 2.8). Basically, misregistration is misrepresentations of tissue structures caused by

a variety of mechanisms, in this case, data acquisition errors during the process of transforming the different sets of data into one coordinate system.

Optimization of the hardware may help to eliminate the artefacts. Most clinical scanners which include self-shielded gradient coil minimizes flux penetration into other conducting elements. This reduces the eddy currents. The form of the gradient waveforms can also be modified to compensate for residual eddy currents. However, this method requires on-site calibration by the field engineer. Parrallel imaging techniques can also further reduce distortions due to eddy currents (Storey, 2006; Koch and Norris, 2005; Norris, 2005; Hiwatashi and Zhong, 2005).

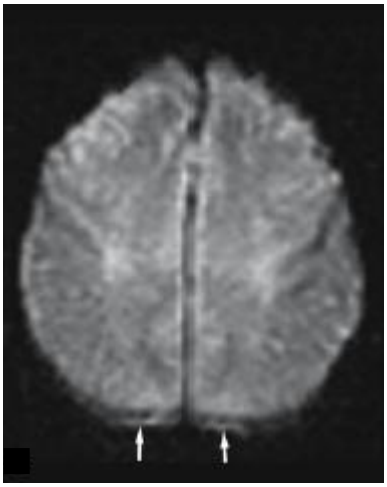

Figure 2.8: Misregistration due to eddy currents in a diffusion-weighted image (Hiwatashi and Zhong, 2005)

(b) N/2 Ghosting Artefacts (Nyquist Ghost)

N/2 ghosting artifact occurs due to phase error in the rephasing-dephasing cycle of the rapidly switching bipolar frequency-encode gradient. For instance, time delays between the imaging gradients and the RF receiver can produce misalignment of the even and odd echoes. While imperfections in the gradient pulses can alter the k-space trajectory, owing to the finite

inductive rise times of the gradient coils and eddy currents in the hardware. The phase error is caused by hardware imperfections. The ghost in these artefacts is always shifted by half of the FOV in the phase-encoding direction. The degree of ghosting often depends on the diffusion gradient pulse (Koch and Norris, 2000).

The severity of the ghost can be diminished by reducing eddy currents as stated in 2.5.2 (a) and adjusting the gradients and magnetic field homogeneity. The artefacts can be further suppressed using higher b value and Fluid Attenuated Inversion Recovery (FLAIR) DWI (Hiwatashi and Zhong, 2005; Storey, 2006). The artefacts can sometimes be reduced using multi-echo reference scan (Schmithorst *et al.*, 2001). Examples of the image artefacts are illustrated in Figure 2.9 (a). Figure 2.9 (b) shows the N/2 ghosting artefacts found in the image obtained in this study. However, it is observed that after making some improvements on the arrangement of the blood sample tubes, this artefacts does not affect the ADC values in the study because it does not overlay on the actual image.

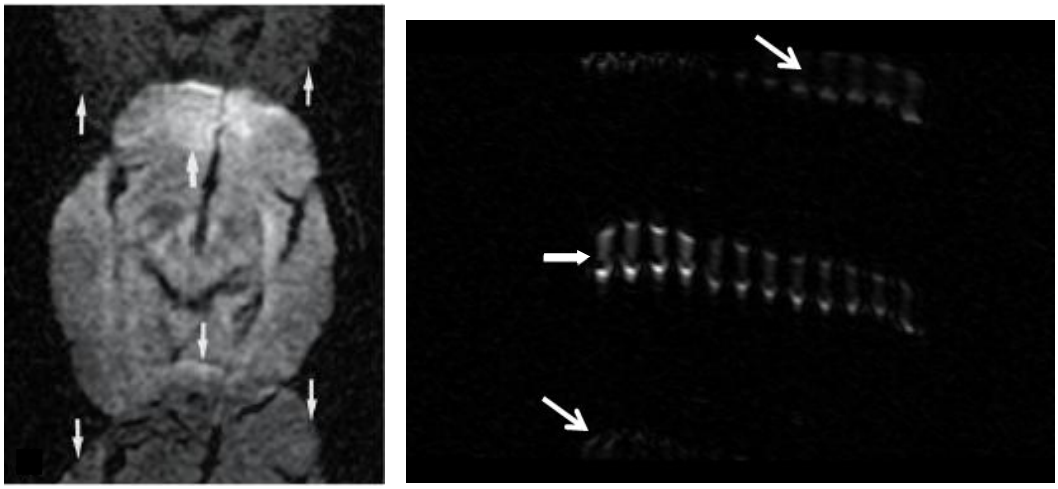

(a) (b)

Figure 2.9: N/2 ghosting artefacts. (a) A DW image of brain with N/2 ghosting artefacts (Hiwatashi and Zhong, 2005) (b) The artefacts were found in the image obtained in this study. The image was shifted by half of the FOV in the phase-encoding direction (open arrow). A distortion (solid arrow) was also seen in the image. However, it is observed that after making some improvement, this artefact does not affect the ADC values in the study because it does not overlay on the actual image.

(c) Susceptibility Artefacts

EPI is sensitive to tissues with different susceptibilities which alters the strength of the magnetic field, resulting in very severe distortion (Figure 2.10). The artefacts are commonly seen at the boundary of tissues with different susceptibilities, such as between the air-filled cavities and surrounding tissues in the head. Susceptibility artefacts are more severe along the phase-encoding direction (Stadler *et al*, 2007).

Use of method that widen the bandwidth in the phase-encoding direction, for instance parallel imaging and interleaved segmentation may help to lessen the artefacts. Another method is undersampling of k-space that may enable an effective bandwidth and shorten readout time, results in thin section and high-resolution matrix (Hiwatashi and Zhong, 2005; Storey, 2006; Stadler *et al*., 2007).

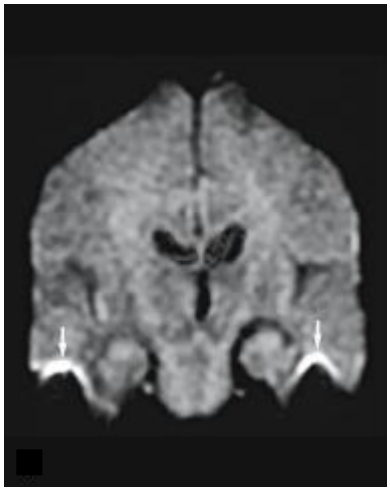

Figure 2.10: Susceptibility artifact in coronal DW image. The region near the mastoids was distorted and appeared hyperintense (Hiwatashi and Zhong, 2005)

2.5.3 Physiology and Subject-Related Artefact

(a) Motion Artefact

Most common artefacts seen in MR image is motion artefacts (Figure 2.11). The sources of motion artefacts include gross head motion, respiratory motion and cardiac-related pulsation. The appearance of the artefacts depend on the motion, i.e whether it is random or periodic. Random motion causes an image blurring while periodic motion commonly causes ghosting due to disruption of the phase encoding process. The artefacts also depend on the specific imaging sequence used. For instance, in order to achieve sufficient diffusion weighting in DWI long gradient pulses have to be applied, which may increase sensitivity to motion.

The most commonly proven method of correction is by utilising high gradient amplitude but reduce gradient pulse duration in DWI. Use of navigator echoes, which is a post-processing technique may help to correct for phase error. Basically, navigator echoes is a technique which consists of special MRI pulse sequences that track the motion of for example, the

diaphragm. Sedation or Periodically Rotated Overlapping Parallel Lines with Enhanced Reconstruction (PROPELLER) techniques are useful in dealing with uncooperative patients. Essentially, PROPELLER imaging is an MRI data acquisition and reconstruction technique in which several k-space lines is acquired in each TR and forming a blade. The blade of a PROPELLER act as rotating wings which rotate around its center to cover the k-space (Arfanakis *et al.*, 2008).

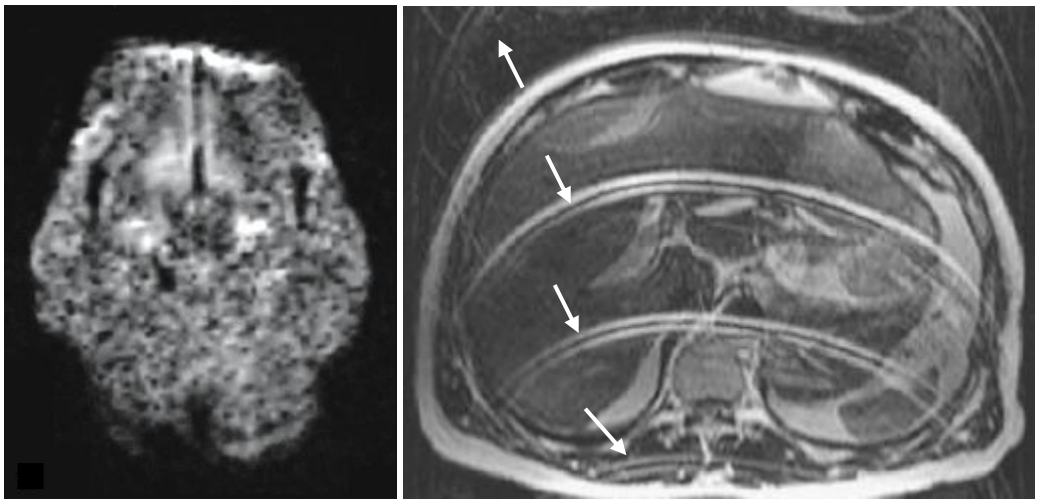

(a) (b)

Figure 2.11: (a) Severe motion artefacts were observed in the DW brain image. The whole data is corrupted by head motion during the scan (Hiwatashi and Zhong, 2005) (b) Ghosting artefacts which occur due to periodic breathing (Stadler *et al.*, 2007)